THE ASTROPHYSICAL JOURNAL, 466:686–694, 1996 August 1

MEASUREMENT OF THE ELEMENTAL ABUNDANCES IN FOUR RICH CLUSTERS OF GALAXIES. I. OBSERVATIONS

R. MUSHOTZKY, M. LOEWENSTEIN,[1] AND K. A. ARNAUD[2]
NASA Goddard Space Flight Center, Code 666, Greenbelt, MD 20771
T. TAMURA, Y. FUKAZAWA, AND K. MATSUSHITA
Department of Physics, University of Tokyo, 7-3-1 Hongo, Bunkyo-ku, Tokyo 113, Japan
K. KIKUCHI
Department of Physics, Tokyo Metropolitan University, 1-1 Minami-Ohsawa Hachioji, Tokyo 192-02, Japan
AND
I. HATSUKADE
Faculty of Engineering, Miyazaki University, 1-1 Gakuen-Kibanadai-Nishi, Miyazaki, 889-21, Japan
Received 1995 June 5; accepted 1996 February 8

ABSTRACT

The elemental abundances of O, Ne, Mg, Si, S, Ca, Ar, and Fe for four clusters of galaxies (Abell 496, 1060, 2199, and AWM 7) are determined from X-ray spectra derived from *Advanced Satellite for Cosmology and Astrophysics* performance verification phase observations. Since the gas in the outer parts of the cluster is optically thin and virtually isothermal, the abundance analysis is very straightforward compared to the analysis of stellar or H II region spectra. We find that the abundance ratios of all four clusters are very similar. The mean abundances of O, Ne, Si, S, and Fe are 0.48, 0.62, 0.65, 0.25, and 0.32, respectively, relative to solar. The abundances of Si, S, and Fe are unaffected by the uncertainties in the atomic physics of the Fe L shell. The abundances of Ne and Mg and to a lesser extent O are affected by the present uncertainties in Fe L physics and are thus somewhat more uncertain. The Fe abundances derived from the Fe L lines agree well with those derived from the Fe K lines for these clusters. The observed ratio of the relative abundance of elements is consistent with an origin of all the metals in Type II supernovae. The presence of large numbers of Type II supernovae during the early stages of evolution of cluster galaxies is a very strong constraint on all models of galaxy and chemical evolution and implies either a very flat initial mass function or bimodal star formation during the period when most of the metals were created.

Subject headings: galaxies: abundances — galaxies: clusters: individual (Abell 496, Abell 1060, Abell 2199, AWM 7) — X-rays: galaxies

1. INTRODUCTION

The detection of Fe line emission from the X-ray–emitting hot intracluster gas (Mitchell, Ives, & Culhane 1975; Serlemitsos et al. 1976; Mushotzky et al. 1978) in virtually all clusters of galaxies (Yamashita 1992) indicates that a significant fraction of the gas has been processed in stars. Relatively large samples of clusters (Yamashita 1992) show that the Fe abundance is narrowly distributed around a mean value of ~ 0.3 solar (Fig. 1) [where the solar abundance of Fe is defined as $\log (\mathrm{Fe/H}) = -4.33$ by number]. Recent spatially resolved spectra of clusters (Ohashi et al. 1995; Mushotzky 1995) show that, except in a few cases, the Fe abundance is relatively uniform out to radii of ~ 1 Mpc and in the case of Coma (Hughes et al. 1993), perhaps to 2 Mpc. Because the mass of the gas exceeds the mass in stars by factors of 2–10 (Henriksen & Mushotzky 1985; David, Forman, & Jones 1995), the implied total mass of Fe is rather large. As shown by many authors (see Arnaud 1995 for a recent review and Renzini et al. 1993 for a detailed analysis), this very large amount of Fe in the intracluster medium places extremely strong constraints on the origin of metals in elliptical galaxies and on virtually all models for the evolution of these systems.

The correlation of total Fe mass with total light from elliptical galaxies (Arnaud et al. 1992) and total iron mass considerations (Renzini et al. 1993) have resulted in a consensus that the metals in the intracluster medium (ICM) originated from elliptical galaxies and that the metals were driven out into the ICM by supernovae–driven winds. The best-fitting models require a large number of Type I or Type II Supernovae (SNs) (Renzini et al. 1993) occurring early on in the "life" of the galaxy. The required SN rate seems inconsistent with a normal Salpeter initial mass function (IMF) and may produce too much light for the available constraints on the luminosity of high-redshift galaxies (Franceschini et al. 1995). One of the main controversies is the relative importance of Type II versus Type I SNs in the production of the observed ICM metals. It is very difficult to calculate this from first principles, since it is a sensitive function of models of stellar evolution, galaxy formation, and the nature of the stars in elliptical galaxies. While recent theoretical work seems to favor SN II's as the primary origin of the metals, the situation is by no means clear (Renzini et al. 1993), since the recent Broad Band X-Ray Telescope (BBXRT) and *Advanced Satellite for Cosmology and Astrophysics* (*ASCA*) results on the metallicity of the gas in elliptical galaxies (Serlemitsos et al. 1993; Awaki et al. 1994; Mushotzky et al. 1994; Loewenstein et al. 1994) are in strong disagreement with most of the theoretical models that assume the empirically estimated SN I rate (Ciotti et al. 1991).

One of the best ways to determine the origin of the metals (Renzini et al. 1993) is to derive the relative abundances of

[1] Also Universities Space Research Association.
[2] Also University of Maryland.

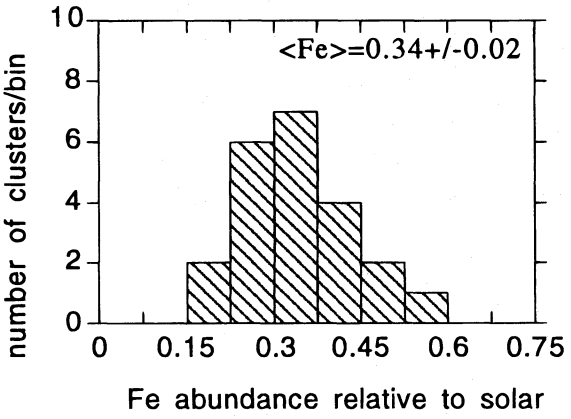

FIG. 1.—Fe distribution for rich clusters of galaxies derived from *Ginga* data.

the elements. Since SNI's essentially produce only Fe (see Timmes, Woosley, & Weaver 1995) while SN II's produce the α-process elements as well, a sensitive measure of the ratio of Type I to Type II supernovae is the relative abundance of the α-process elements (O, Ne, Mg, Si, and S) compared to Fe. Preliminary results on the abundances of these elements in the ICM were obtained for a few objects with the instruments on the *Einstein Observatory* (Mushotzky et al. 1981; Canizares et al. 1982; Rothenflug et al. 1984) and indicated that O/Fe ~ 3 solar and Si/Fe ~ 2 solar. However, these results were obtained for the centers of clusters with cooling flows, where the thermal model is rather uncertain, producing rather large systematic errors on the abundances. There were also attempts to derive elemental abundances from the optical line ratios in cooling flows in clusters (Hu, Cowie, & Wang 1985), but, because of the great uncertainty in the ionization mechanism for this gas, the errors in these results are difficult to quantify.

ASCA (Tanaka, Inoue, & Holt 1994) X-ray spectral observations of clusters provide the first opportuntity to determine the elemental abundances for the bulk of the ICM in clusters (Mushotzky 1995) and determine the origin of these elements. In this paper we present an analysis of the elemental abundances of the four brightest, moderate temperature clusters observed by *ASCA* in the performance verification (PV) phase. These objects have very simple morphologies and do not show evidence for sharp abundance gradients (see Ohashi et al. 1995). In order to increase the signal-to-noise for an accurate determination of the relatively weak lines due to the alpha burning elements, we have analyzed the integral spectra and leave the differential analysis to later work. An extensive theoretical discussion of the implications of these results is included in the companion paper (Loewenstein & Mushotzky 1996).

2. MODELING CONCERNS

Because of the strong dependences of line equivalent width on temperature and the present uncertainty in Fe L-shell atomic physics for temperatures less than 2 keV (Fabian et al. 1994; Liedahl, Osterheld, & Goldstein 1995), one is restricted to clusters with $2.5 < kT < 5$ keV to derive the abundances of the alpha burning products (O, Ne, Mg, Si, S, Ca, Ar) via use of K shell transitions while also using K shell lines to derive the Fe abundances. The atomic physics of the He and H-like K lines of these elements is very straightforward, and the predictions of the collisional equilibrium codes (Raymond & Smith 1977; Mewe & Kaastra 1992) should have little error and agree well with each other. Since the gas in the outer parts of the cluster is optically thin and in the low-density limit of coronal equilibrium, and the effects of dust are minimal in the X-ray band, the analysis is very straightforward compared to the analysis of stellar or H II region spectra, where the effects of radiative transfer, dust, and ionization balance are very complex and difficult to remove accurately. In many respects, it is easier to derive the abundances from X-ray imaging spectra of the ICM in clusters than in any other field of astrophysics.

For clusters with $2.5 < kT < 5$ keV, the abundances for O, Ne, Mg, Si, S, Ca, and Ar are primarily determined from the H-like line strengths for which the atomic physics should be well understood, and the lines of most of these elements are strong enough to be measured by *ASCA* with a deep enough exposure for a bright enough object. The Fe abundance is primarily obtained from analysis of the He-like line (which occurs near 6.67 keV) strengths for clusters in this temperature range. We stress that, with *ASCA*, we directly measure the temperature of the continuum radiation that is responsible for the collisional excitation of the gas and do not have to rely on indirect measures of the ionization of the lines.

However, the predicted abundances in a coronal plasma are sensitive functions of the continuum temperatures (see Mushotzky 1984, Fig. 5). In a collisonal equilibrium plasma in the temperature range 1–8 keV, the equivalent width of the hydrogen-like lines of the alpha burning elements is roughly proportional to $kT^{-3/2}$. All of these lines are rather weak. For example for a 1/2 solar abundance gas, the predicted EWs of the Lyα H-like line from Si and S are only 50–75 eV at $kT \sim 1$–2 keV, and for a 4 keV continuum temperature, the EW of the Ne H-like line is only 6 eV. Thus, it is very difficult to determine elemental abundances of the low-Z elements for the hotter clusters using a detector with the *ASCA* SIS detector spectral resolution of ~60 eV at 1 keV.

Additional problems arise from uncertainty in the Fe L atomic physics, since some of the stronger Fe L lines due to Fe XXII and Fe XXIV are quite close to the H-like lines of Ne and Mg, respectively. Simulations of solar abundance thermal plasmas show that for $kT \sim 4$ keV, the EW is ~11 eV for the 1.022 keV H-like Ne line, while the Fe XXII blend at 1.129 keV has an EW of ~90 eV. Thus, modeling of the much stronger Fe L blend, only 1.5 spectral resolution elements away from the Ne line, is of some concern. The situation for Mg is worse, with a strong line of Fe XXIV at 1.49 keV (EW ~25 eV for solar abundances) compared to the $E \sim 1.472$ keV for H-like Mg, which has a predicted EW of 15 eV. Since we know that there are errors in the relative strengths of the Fe XXIV lines in the Raymond-Smith and MEKA plasma codes (Liedahl et al. 1995), it seems inevitable that the true errors in the Mg abundance will be larger than the statistical ones. The situation for oxygen is also difficult because of its low EW for continuum temperatures hotter than 2 keV. At a continuum temperature of $kT \sim 4$ keV, the predicted H-like oxygen EW is ~30 eV and the detector resolution is ~60 eV. In addition, there is sensitivity to the exact values of the absorbing column density. Simulations of a $kT = 4$ keV cluster with galactic absorption of 3×10^{20} atms cm^{-2} and 0.3 solar abundance shows that the column density and oxygen abundance are corre-

lated and that a 1×10^{20} atm cm^{-2} uncertainty in the column translates to a factor of 2 error in the oxygen abundance. However, if the oxygen abundance is solar (with the same galactic column density), the errors in abundance and column density are not strongly coupled, and the same error in N(H) results in only a 30% error in oxygen abundance.

Recently (Mewe & Kaastra 1995), a new version of the "MEKA" code (called MEKAL) has been developed that incorporates a large amount of new atomic data and revisions of the ionization balance. In particular (Leidahl et al. 1995), predictions of the strengths of the Fe XXIV lines are much improved. Since it is these lines that have the largest impact on the Mg abundance determinations, we have simulated the effect of fitting a "MEKAL" plasma of $kT = 4$ keV with the R-S code. We find virtually no effect for observations with the signal-to-noise ratio presented in this paper. If the signal-to-noise is increased by a factor of 10, there is a small, $\sim 10\%$, effect on the Ne abundance, but the Mg abundance is not affected. We conclude that with our present knowledge of the Fe L atomic physics, the results presented here are not strongly affected by uncertainties in the Fe L lines and the additional systematic uncertainties in the Mg and Ne abundances are not large.

The silicon and oxygen abundances are sensitive to the uncertainties in the SIS (solid state imaging spectrometer; Tanaka et al. 1995) detector response function because of the presence of oxygen and silicon absorption features in the detector and its window. We have attempted to estimate the size of the systematic error via the use of several different detector response functions. Since the start of the PV data analysis two years ago, four different detector response functions have been released. While the changes between these response functions are subtle, the differences reflect uncertainties in the details of the detector and telescope efficiencies and energy redistribution matrix and in some sense span a wide range of possibilities. The fact that the variance in the abundance analysis from response function to response function is less than the statistical error in the oxygen abundance (the element most sensitive to variations in the response matrix) gives confidence in the robustness of the analysis. These different fits indicate that there may exist at most $\sim 30\%$ uncertainty in the Si abundance due to uncertainty in the response functions.

As will be seen below, we derive moderately small errors for Ne and O abundances and large uncertainties in the Mg abundances. Based on the simulations, this indicates that the supersolar ratios of O/Fe or Ne/Fe are real, but that, despite the good agreement between the MEKAL and R-S simulations, the uncertainties in the Fe L physics and detector dominate the error in the Mg abundance. For Si the statistial errors are smaller than the systematic errors.

3. CLUSTER SELECTION AND ANALYSIS

Because of the arguments given above, we have selected the four brightest clusters observed during the *ASCA* PV phase with temperatures between 2.5 and 5 keV and for which the central cooling flow region can be well subtracted from the data. This selection gives four objects: Abell 496, Abell 1060, Abell 2199, and AWM 7. All these clusters have measured kTs from *Ginga* (Yamashita 1992; Tsuru 1993; Hatsukade 1989) between 2.5 and 4.22 keV and have total fluxes derived from big beam measurements of (6–8) $\times 10^{-11}$ ergs cm^{-2} sec^{-1} in the 2–10 keV band. We have not analyzed the data for Hydra A or MKW3s, the other clusters with similar temperatures observed during the PV phase, because these objects are a factor of 2 dimmer, and the resulting errors on the abundances are considerably larger. In addition, we have not analyzed Abell 1795 in detail for this paper, because its 5.3 keV temperature results in larger errors for O and Ne.

For all of these systems, we have removed a ring 3′ in radius from the center to eliminate possible contamination from a cooling flow or from a possible abundance gradient (Ohashi et al. 1995) and have analyzed data out to a radius of $\sim 11'$, corresponding to the field of view of the SIS (a $22' \times 22'$ square). All the clusters were observed in 4-CCD mode. We believe that the exclusion of a ring of this size is a conservative way of eliminating the effects of a cooling flow. For three-quarters of the clusters, the measured cooling radius (~ 170 kpc for A2199 and A496 and 110 kpc for AWM 7; Arnaud 1986) corresponds to $\sim 3'$. A standard cooling flow model, in which the mass dropout rate is proportional to the radius, convolved with the *ASCA* point-spread function (PSF), gives very little flux, less than 5% of the total cooling flow component, at $R > 3'$ for these clusters. This flux is less than 2% of the total cluster emission in the 3′–11′ ring. For A1060, the inferred cooling rate is very low, and there is no evidence in the *ASCA* spectra for lower temperature emission. The final spectra are all of very high quality, with more than 50,000 counts in each of the SIS cameras. Fits to isothermal models with variable abundances result in somewhat high, but acceptable, χ^2/ν (Table 1) and have no systematic residuals indicative of multitemperature plasmas. We note that for three-quarters of the systems, the *ASCA* temperature (Table 1) and the *Ginga* result are in excellent agreement. For A1060 the *Ginga* kT value of 2.55 keV for a two-temperature fit to the cluster is not consistent with the *ASCA* kT value of 3.2 keV, but the isothermal fit of $kT = 3.55$ keV (Hatsukade 1989) is in fair agreement. We also find (compare Tables 1 and 2) that the Fe abundances derived from the *ASCA* and *Ginga* data are in good agreement when corrected for the solar Fe abundance of 4.68×10^{-5} used in the present analysis, as opposed to the value of 4×10^{-5} used in the original *Ginga* analysis.

We have used a circular annulus for each cluster centered on the peak of the X-ray emission and have used deep sky background selected from the same regions of the detector. Because the clusters fill the field of view of both detectors, it is not possible to use the same fields to subtract background. The data were cleaned in the usual fashion, and both the source and the background were selected to have cutoff rigidity greater than eight to minimize the effects of background subtraction at high energies. For these bright clusters, background subtraction is only important at $E > 7$ keV and at $E < 0.8$ keV. At $E > 7$ keV, internal background dominates and the main effect of "incorrect" background subtraction for these intermediate-temperature clusters is to increase the fitted χ^2 rather than change the temperature. At $E < 0.8$ keV, the main background component is due to galactic emission (Gendreau et al. 1995) and the main effect is a fitted column density that disagrees with the galactic value. Neither of these effects produces significant variance in the derived abundances. Data were grouped such that each channel had a minimum of 25 counts so that the χ^2 statistic could be utilized. The GIS data were fitted in the 0.7–10 keV band and the SIS data in

the 0.4–10 keV band. The differing numbers of degrees of freedom in each fit represent the results of the binning process and are related to the counting rates, exposure time, and temperature of the cluster.

In order to check whether the abundance variations are due to possible errors in the detector calibrations, we have analyzed the GIS and SIS data separately. We have used the ray model in the 1994 release of XSPEC, which has the following solar number abundances relative to hydrogen: O:Ne:Mg:Si:S:Ar:Ca:Fe:Ni-(85.1, 12.3, 3.8, 3.55, 1.62, 0.36, 0.229, 4.68, 0.179) $\times 10^{-5}$. In this model, the redshift of the cluster was fixed at the optical value, which is consistent (Mushotzky 1995) with the redshift derived from fitting the X-ray spectra. With the exception of Mg, the abundances are not correlated with each other, nor are they strongly coupled with the fitted continuum temperature (see Fig. 2 below), and thus we have used $\chi^2 + 2.706$ errors (90% confidence for one interesting parameter).

As discussed above, the Mg abundances are correlated with the Fe abundances. Despite the strong correlation of equivalent width of the H- and He-like lines of the abundant elements and continuum temperature for collisional equilibrium plasmas, the very small *ASCA* uncertainties in temperature serve to minimize the derived errors in abundance. In addition, because of the good *ASCA* spectral resolution, the line strengths and the continuum temperature are not observationally correlated, in contrast to previous results obtained with proportional counters. Carbon and nitrogen are very difficult to measure with *ASCA* because of the relatively low resolution of the SIS at $E < 0.5$ keV, where the H-like lines of these elements appear. Also, these elements have lower ionization potentials and the equivalent widths are very low at the temperatures of interest in clusters. For example, the upper limits on the N abundance in A2199 and A496 are 2.5 and 8 times solar, respectively. For the purposes of our analysis, we have assumed that carbon and nitrogen have 0.3 solar abundances, while He has a solar abundance. The derived abundances of the other elements are insensitive to the carbon and nitrogen abundances but are sensitive to the He abundance. This is because the abundance is basically determined by the equivalent width of the observed lines compared to the "bremsstrahlung" continuum. Since the strength of the continuum is a function of the number of free electrons and since He is the main contributor, after hydrogen, to the free electron population in an ionized plasma, the abundance of the heavier elements depends inversely on the He abundance.

4. RESULTS

We show in Table 1 the temperatures and fluxes, in Table 2 the abundances for each cluster from the SIS data, and in Table 3 the GIS abundances. The error ranges given are 90% confidence for one interesting parameter. In Figure 2 we show selected error contours for elemental abundances to give the reader an idea of the statistical uncertainties, and Figure 3 displays the overall spectral fits for A496. In Figure 4 we show the residuals in the region from 0.5–3 keV to

TABLE 1

TEMPERATURES AND χ^2 FOR *ASCA* SIS SPECTRAL FITS TO CLUSTERS AND *Ginga* VALUES FOR kT AND Fe ABUNDANCES

Cluster Name	kT(*ASCA*)[a]	χ^2/ν	Flux in Field of View[b]	kT(*Ginga*)[c]	Fe Abundance (*Ginga*)[d]
Abell 496.....	4.17 (3.99–4.23)	621/422	2.4	3.97 ± 0.06	0.32 ± 0.05
Abell 1060.....	3.02 (2.97–3.08)	579/439	2.7	3.27 ± 0.051[e]	0.34 ± 0.04
Abell 2199.....	4.17 (4.06–4.28)	540/408	3.6	4.48 ± 0.06	0.29 ± 0.04
AWM 7	3.56 (3.48–3.63)	573/442	4.8	3.89 ± 0.15	0.42 ± 0.10

[a] The *ASCA* errors are 90% confidence errors.
[b] Flux is in the 2–10 keV band in units of 10^{-11} ergs cm^{-2} s^{-1}.
[c] *Ginga* data from White et al. 1994 for A496 and A2199, Hatsukade 1989 for A1060, and Tsuru 1993 for AWM 7.
[d] The *Ginga* values have been renormalized to a Fe value of 4.67×10^{-5} from the values used in the original paper.
[e] Yamashita 1992 quotes a two-temperature fit with $kT_1 = 2.55 \pm 0.04$ and $kT_2 = 7.37 \pm 0.49$.

TABLE 2

CLUSTER ABUNDANCES WITH RESPECT TO SOLAR VALUES (SIS DATA ONLY)

Cluster Name	O	Ne	Mg	Si	S	Ar	Ca	Fe	Ni
Abell 496.....	0.67 (0.34–1.11)	0.914 (0.60–1.28)	0.47 (0.18–0.78)	0.56 (0.39–0.74)	0.32 (0.13–0.52)	0.32 (<0.77)	0.26 (<0.72)	0.33 (0.29–0.395)	1.46 (0.85–2.11)
Abell 1060	0.34 (0.19–0.49)	0.57 (0.41–0.72)	0.20 (0.5–0.36)	0.57 (0.48–0.66)	0.23 (0.13–0.33)	0.02 (<0.24)	0.0 (<0.23)	0.28 (0.25–0.38)	0.69 (0.19–1.65)
Abell 2199	0.44 (0.18–0.71)	0.67 (0.38–0.97)	0.46 (0.17–0.78)	0.926 (0.73–1.1)	0.279 (0.08–1.10)	0.0 (<0.25)	0.0 (<0.39)	0.348 (0.31–0.39)	1.19 (0.50–1.75)
AWM 7	0.48 (0.21–0.77)	0.34 (0.12–0.57)	0.0 (<0.2)	0.53 (0.41–0.66)	0.19 (0.06–0.33)	0.0 (<0.15)	0. (<0.19)	0.336 (0.30–0.37)	0.752 (0.31–1.21)
Average	0.48	0.62	...	0.65	0.25	...	...	0.32	1.02
SN II abundances[a].....	1.0	0.94	1.7	0.85	0.43	0.31	0.36	0.26	...
SN I abundances[b]	0.037	0.016	0.090	0.55	0.56	0.60	1.6	1.0	...

NOTE.—All errors are 90% confidence uncertainties.
[a] Abundances from 20 $M_\odot$ Type II SN from Thielmann, Nomoto, & Hashimoto 1996, normalized such that O = 1.
[b] Normalized such that Fe = 1 (Nomoto, Thielmann, & Yokoi 1984).

TABLE 3

CLUSTER ABUNDANCES WITH RESPECT TO SOLAR VALUES (GIS DATA ONLY)

Cluster Name	Si	S	Ar	Ca	Fe	Ni
Abell 496.....	0.85	0.41	0.0	0.91	0.34	0.22
	(0.54–1.18)	(0.06–0.77)	(<0.74)	(0.12–1.69)	(0.29–0.39)	(<1.34)
Abell 1060.....	0.56	0.28	0.02	0.22	0.35	0.09
	(0.38–0.77)	(0.08–0.50)	(<0.37)	(<0.67)	(0.30–0.41)	(<0.98)
Abell 2199.....	1.32	0.29	0.0	0.0	0.32	1.50
	(0.75–1.32)	(<0.6)	(<0.71)	(<0.85)	(0.29–0.37)	(0.44–2.6)
AWM 7	0.76	0.60	0.0	0.31	0.39	1.95
	(0.32–1.00)	(0.34–0.88)	(<0.39)	(<0.90)	(0.35–0.44)	(0.95–2.98)

NOTE.—All errors are 90% confidence uncertainties.

demonstrate the presence of emission lines from O, Ne, Fe L, Si, and S.

One immediately notices that, with the possible exception of Si in Abell 2199 and Fe in Abell 1060, the abundances of all of these clusters are similar to each other, within statistical errors, and that the abundances of O, Ne, and Si tend to be twice the relative abundance of S and Fe. This confirms the preliminary analysis of these data presented in Mushotzky (1995). Because of the relatively large uncertainties in all the metals (except Fe), we have not attempted to determine whether there exists a relative abundance gradient in these systems. Very similar results for the clusters

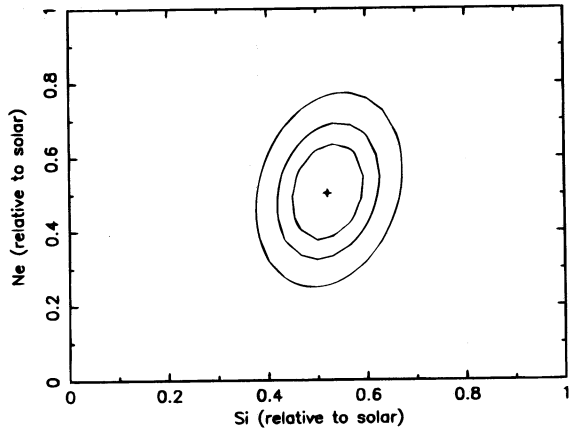

FIG. 2a

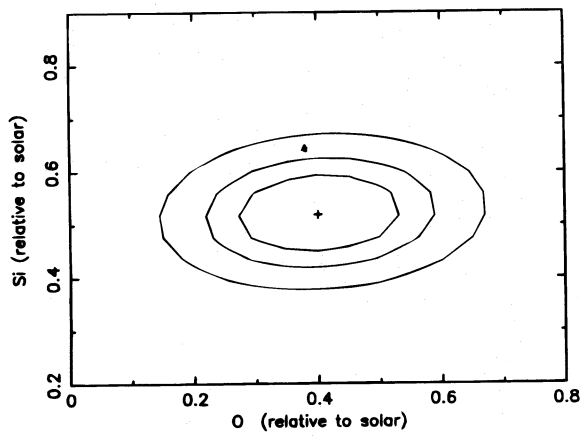

FIG. 2b

FIG. 2.—Probability diagrams for the uncertainty in selected abundances for Abell 1060. The three contours correspond to $\chi^2 + 2.3$, 4.61, 9.21, which correspond to 68%, 90%, and 99% confidence contours, respectively, for two interesting parameters. The contours are "round," indicating that the value in each interesting parameter is not coupled with the other parameters. The best-fit values are indicated by a plus. Notice that the size of the 68% contours are considerably smaller than the $\chi^2 + 2.706$ errors given in Tables 2 and 3.

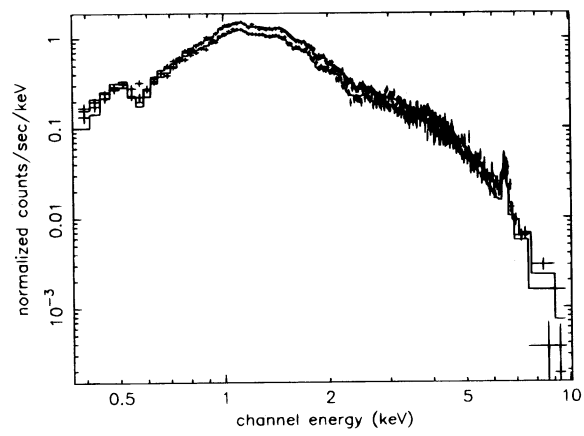

FIG. 3a

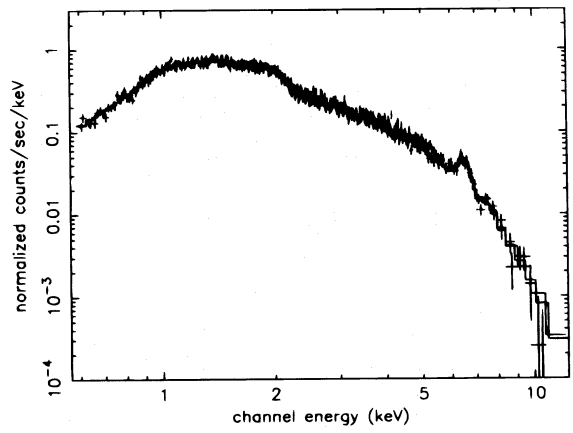

FIG. 3b

FIG. 3.—Overall spectral fits for the SIS and GIS for Abell 496. The *y*-axis corresponds to detector units and the solid line corresponds to the best-fitting variable abundance model.

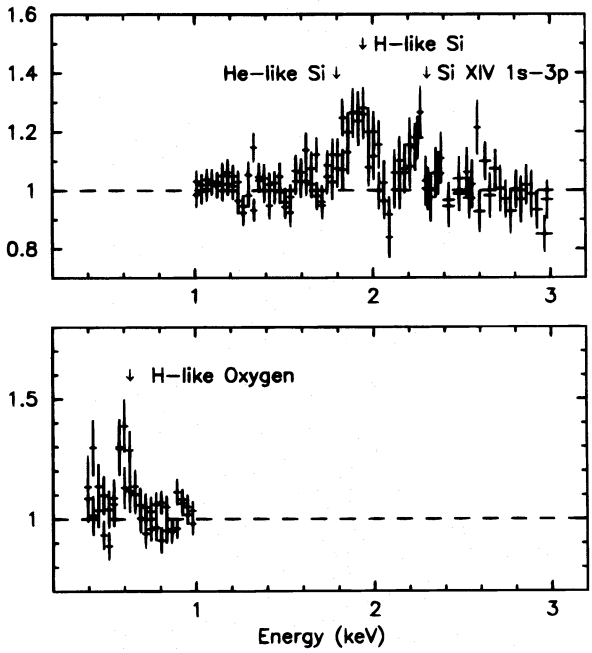

FIG. 4a

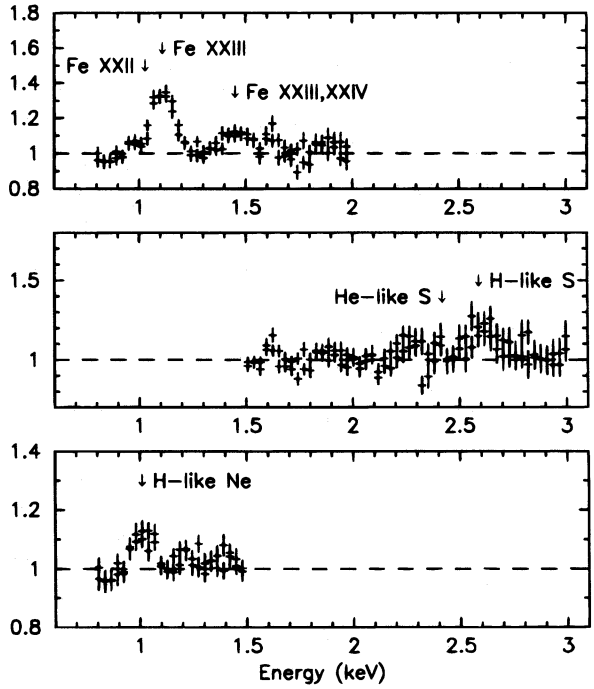

FIG. 4b

FIG. 4.—Ratio of the data to the model for selected spectral regions in (*a*) Abell 2199 and (*b*) Abell 1060. These plots were made by finding the best fitting variable abundance models and then setting the values of the selected elements to zero and then plotting the ratio. This plot is designed to show which spectral features have dominated the fitting for which elements.

are also found with the use of the Mewe & Kaastra (1992) code (the Meka model in XSPEC).

The GIS is not capable of measuring the abundances of O, Ne, and Mg because of its poorer spectral resolution and available bandpass. Also, because of its poorer resolution, it is less sensitive to the weak spectral lines. For all practical purposes, the GIS data can only tightly constrain Si and Fe and, somewhat more poorly, S, Ca, Ar, and Ni. As can be seen in Table 4 and Figure 5, the derived abundances are in excellent agreement with the SIS abundances. This is important because the GIS and SIS detectors have rather different spectral responses. In particular, the GIS detector does not have a Si edge near 1.8 keV, and the SIS detector does not have a Xe spectral feature near 4.7 keV. Combination of the two sets of detectors does reduce the errors somewhat; however, we prefer, at this stage of the *ASCA* calibration process, to treat the two detectors as separate and confirming measurements of the elemental abundances.

However, as an example, we calculate the uncertainty in the Si, S, Ca, and Ar abundances when we use the SIS and GIS data together for A2199. We find Si = 0.83 (0.68–0.99), *S* = 0.26 (0.097, 0.44), Ar = 0.0 (<0.16), and Ca = 0.22 (0.0, 0.63), reflecting a mean reduction in uncertainty of greater than 20%.

A question of interest for determining the sensitivity to thermal models of the cluster and for the reliability of the atomic physics used is the Fe abundance derived using Fe L lines (predominantly due to Fe XXII, Fe XXIII, and Fe XXIV, the strongest Fe L lines at these temperatures, Fig. 4) compared with that derived from Fe K (Table 4). We find that these abundances agree very well within the uncertainties

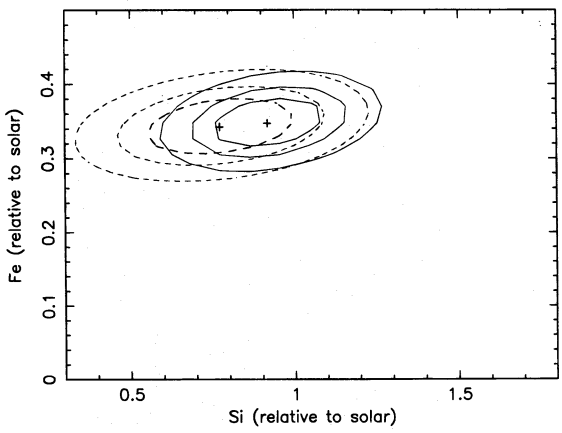

FIG. 5.—Comparison of the error contours for the uncertainty in Si and Fe for the SIS and GIS detectors for Abell 2199. The GIS contours are the dashed lines and the SIS contours are the thin solid lines. The contours correspond to the values in Fig. 2.

TABLE 4

Fe K VERSUS Fe L SHELL ABUNDANCES

Cluster Name	Fe K	Fe L
Abell 496	0.30 (0.26–0.35)	0.26 (0.20–0.33)
Abell 1060.....	0.23 (0.20–0.26)	0.28 (0.25–0.31)
Abell 2199.....	0.348 (0.31–0.39)	0.29 (0.21–0.37)
AWM 7	0.302 (0.26–0.41)	0.31 (0.26–0.36)

NOTE.—All errors are 90% confidence uncertainties.

(Table 2) and that, at least at these temperatures, there are no major systematic differences between the Fe L to Fe K line abundances, indicating that the Fe L line strengths from the Meka and Raymond-Smith plasma codes are approximately correct for this temperature range. This test is also sensitive to the thermal model. If there was a significant emission measure of cooler gas, due, for example, to scattering of the cooling flow spectra into the 3′–11′ rings, the observed Fe L lines would be considerably stronger (see Fabian et al. 1994) than if they were due solely to the hot component. The fact that the Fe L abundances agree well with the Fe K values indicates that the contribution of lower temperature gas is small and that the influence of temperature structure on the elemental abundances is weak. In addition, since the strongest observed Fe L lines are due to Fe XXIII rather than Fe XXII or Fe XX (Fig. 4), there exists only a very small emission measure of gas cooler than 2 keV. Recently (Borkowski 1995; Kaastra 1995), preliminary versions of revised collisional equilibrium plasmas models have been released. While these codes are in the test stage, we find that the fitted abundances using these newer codes do not change within the uncertainties.

Analysis of Abell 426 (Arnaud et al. 1994) shows a similar pattern of Si, S, Ca, and Ar versus Fe abundances and a similar pattern in the Si abundance is seen in Abell 1795 (Mushotzky 1995) and MKW3S (Hatsukade, Kawarabata, & Takenaka 1995). These results indicate that the pattern of abundances for the four clusters analyzed here also extends to other objects.

Recently Singh, White, & Drake (1996) have performed a detailed analysis of the abundance pattern derived from *ASCA* observations of AR Lac, a bright star, with signal-to-noise levels similar to those of our clusters. They conclude, after a rather exhaustive discussion of a wide variety of possibilities, that the *ASCA* abundances are robust and statistically reliable. In this observation, the abundance pattern is consistent with the solar ratio except that the Si:S ratio and Ne:Fe is about twice solar. In particular, for their best-fitting model, they do not find a high Si:Fe ratio. Similar results are also found for *ASCA* observations of Algol (Antunes, Nagase, & White 1994), another bright star with high–signal-to-noise ratio data.

5. DISCUSSION

The relatively high abundance of the α-burning products compared to Fe strongly suggests that the gas has been primarily enriched by Type II supernovae (Elbaz, Arnaud, & Vangioni-Flam 1995; Loewenstein & Mushotzky 1996). In addition, the very uniform gas composition of those systems suggests a very homogeneous process. The relatively high gas mass fractions (~20% of the total mass at $R \sim 1$ Mpc in the X-ray–emitting gas for these clusters; White & Fabian 1995), combined with the lack of a sharp metallicity gradient (Ohashi et al. 1995), also requires a large number of supernovae to produce the observed total metallicity. Since each Type II SN of 25 $M_\odot$ (the mass-weighted average mass of Type II SN) produces enough metals to enrich 225 $M_\odot$ of primordial material to solar abundances (Woosley & Weaver 1986), one requires a total of $\sim 10^{12}$ Type II supernovae to have exploded to produce the overall mass of metals in these clusters (see Renzini et al. 1993 for a detailed discussion). Because Type I SNs produce essentially only Fe, the present data also allow a tight upper limit on their total number during the life of the cluster if we assume that all the Si is produced by SN II's. However, this is subject to uncertainty in the slope of the IMF, since the amount of Fe produced in Type II SNs is a strong function of mass, and to uncertainties in the SN II explosion physics, which allows for a factor of 2–3 variation in the Fe yield (for an extensive discussion, see the companion paper by Loewenstein & Mushotzky 1996).

While the overall pattern is quite indicative of Type II SNs, the observed abundance ratios are not in detailed agreement with theoretical models, with S, Ca, and Ar being relatively low in the clusters compared to the models. An extensive discussion of the limits that the observed abundances can place on the IMF and on nucleosynthesis models is contained in the companion paper by Loewenstein & Mushotzky (1996) and we refer the reader to that paper.

Comparison with the abundances in old stars (see the figures in Timmes et al. 1995) shows that at Fe ~0.3 solar the observational scatter is rather large (Gratton & Ortolani 1986), but the pattern is roughly similar to that seen in the clusters with the following ratios with respect to solar: O/Fe ~ 0.8–2, Si/Fe ~ 1.1–2, S/Fe ~ 0.6–3, Ca/Fe ~ 1–1.75, Ni/Fe ~ 1–1.6 (Ar and Ne are not measured in stars). However, somewhat better agreement between the observed cluster abundance ratio data and the stellar data are seen at Fe ~ 0.1 solar, where the ratios of the α-burning products O and Si to Fe are ~2, but the observed S/Fe ratio is also larger than solar, inconsistent with the cluster data. Timmes et al. (1995) note that there is some controversy over the S data (see below).

In their detailed model of chemical evolution of the Milky Way, Timmes et al. (1995) obtained good agreement with the observed stellar abundances as a function of both age and metallicity for a wide variety of elements, but they have constructed a model specific for our Galaxy and whose details certainly are not correct for the rather different evolutionary history of the cluster gas.

One of the major discrepancies with the predicted Type II abundances is the low observed S/Fe ratio compared to the model predictions. This low ratio is also seen in old planetary nebulae (de Freitas Pacheo 1993) and in galaxies (e.g., Henry, Pagel, & Chincarini 1993). The pattern of decreasing S/O with increasing O abundance is seen in most spiral galaxies, and it is suggested that this is because S is produced over a narrower mass range than O (Matteucci & Francois 1989). Inclusion of such an effect in our simple assumption of Type II SNs might account for the S discrepancy noted above. However, the interpretation of these optical data are subject to (possibly) large and uncertain corrections for dust and uncertainties in the form of the stellar ionizing spectrum for planetary nebulae and H II regions in galaxies.

The only other relevant dataset for the comparison of elemental abundances is the relative abundance in the stars in elliptical galaxies. Since these stars are, in general, older than 5 Gyr, and are probably directly related to the stars that have produced the metals now seen in the ICM, they may be more relevant than the old stars in our Galactic halo. The only available data (Worthey, Faber, & Gonzalez 1992) indicate that Mg/Fe ~ 2 solar, also indicative of production by SN II's. However, the abundances of the other elements are not determined.

It is worth noting that the abundances in the overall metal poor Magellanic systems (Russell & Dopita 1992;

Luck & Lambert 1992) have a rather different pattern (Russell & Dopita 1992). As summarized by Luck & Lambert (1992), "oxygen is less abundant in the clouds than in galactic stars of the same (Fe) metallicity." We also note that the Si:Fe ratio is high. Thus, it seems as if massive SN II's in the Clouds have been less important than in our own Galaxy, consistent with the steeper slope of the IMF found for the LMC (Hill, Madore, & Freeman 1994). These results are also consistent with the relative youth of the LMC stars and a longer infall timescale (Dopita 1991).

For a general description of the constraints that the relative elemental abundances impose on models of star formation and evolution see Dopita (1991). Perusal of this paper shows that the observed abundances in the cluster ICM strongly favor models with rather different parameters (such as slope of the IMF and infall timescale) than those derived for our Galaxy. In particular, a shallow slope to the IMF is preferred, opposite to what is inferred for the LMC (see Loewenstein & Mushotzky 1996). This is similar to recent conclusions reached by Mathews (1989), Arnaud et al. (1992), and David et al. (1991). Following the discussion in Dopita (1991), where the ratio of Fe produced by SN I's is related to the infall timescale of the gas, one is led to the view that rapid formation of elliptical galaxies requires either an IMF biased to high-mass stars or one in which, at least initially, low-mass star formation is suppressed (Elbaz et al. 1995; Loewenstein & Mushotzky 1996). As pointed out by many authors, low-mass stars lock up the α-burning elements produced in massive stars and are the progenitors of Type I SNs. Since it seems as if the gas has not been influenced much by SN I's, one is led to the assumption that, for whatever reason, the SN I rate in elliptical galaxies is rather low. It is worthwhile to note that X-ray observations of elliptical galaxies also imply a much lower SN I contribution to the measured metallicity than most theoretical models would assume (Renzini et al. 1993; Awaki et al. 1994; Mushotzky et al. 1994; Loewenstein et al. 1994; Loewenstein & Matthews 1991). The severity of this discrepancy is not clear, pending better data on the present SN I rate in elliptical galaxies and a better understanding of the formation and evolution of the SN I progenitors.

However, according to the calculations of David et al. (1991), the O/Fe ratio is only a very weak function of the SN I rate. This relative constancy of the O/Fe ratio is due to the neglect of a possible variation in the SN I rate with time in their calculations. These authors predict values of O/Fe ~ 2 for a wide range of models, consistent with our observed average abundance of O, Ne, and S with respect to Fe.

A moderately serious problem with the massive burst of star formation postulated to have created the galactic winds is that galaxies are predicted to have an extremely high luminosity during the epoch of metal formation and such luminous galaxies are not seen in sensitive redshift surveys. With a total of $\sim 5 \times 10^9$ Type II supernovae required per $L \sim 10^{11}$ galaxy and a lifetime for the metal producing process of less than 3×10^8 years, the implied luminosity is $\sim 5 \times 10^{13}\ L_\odot$ (Renzini et al. 1993), which, for $H = 50$ and $z = 3$, predicts $M = 20.8$ (ignoring K-corrections and redshift effects), well within the limits of present surveys, from which such objects are absent. Thus, we must conclude that either these objects are dust enshrouded, at much higher redshifts, or have a much longer period of star formation. If the latter, then the timescale for evolution of these systems would be much longer than that consistent with Type II supernova lifetimes and initial bursts of star formation assumed in most models (Franceschini et al. 1995). However, if there is an extended period of star formation, the galactic winds necessary to expel the material out of the galaxies into the intergalactic medium are much less likely to form (Ciotti et al. 1991).

6. CONCLUSIONS

We have determined for the first time the abundances of O, Ne, Si, S, Ar, Ca, and Fe in a sample of clusters. We find that the abundance pattern in each cluster is very similar and is roughly consistent with the origin of most of the metals in Type II SNs (see the companion paper by Loewenstein & Mushotzky 1996). This result is rather contrary to simple theory (see Renzini et al. 1993) and ought to be considered in any theory that seeks to understand the formation and evolution of elliptical galaxies and clusters of galaxies. The galaxies that contain these stars should have been ultraluminous during the epoch of metal generation. The absence of these predicted luminous elliptical galaxies in redshift surveys implies that either these galaxies were dust enshrouded, that the epoch of metal formation was at very high redshift, or that the period of high SN II rate was much longer than assumed by models of spheroid formation. The high total metal mass in α-burning products indicates that, if the present-day elliptical galaxies were responsible for the observed metallicity, these galaxies have lost approximately half of their initial baryonic mass.

While the overall pattern is clear, there are deviations in the abundances of S, Ca, and Ar from those predicted for Type II SNs. Deviations in the opposite direction are seen in the Magellanic Clouds and are in the sense that the cluster data favor a flat IMF or bimodal star formation. It is clear that detailed galactic evolution/nucleosynthesis calculations are required to derive all the information from the present data set. It is somewhat odd that "old" red stellar systems, such as clusters of galaxies, seem to have their metallicity dominated by a flat IMF, while young, blue light–dominated systems such as the Magellanic Clouds are dominated by a steep IMF.

Detailed studies of lower temperature, less massive clusters with *ASCA* are in progress and will be reported in a future paper. These studies are important in refining the nature of the ratio of metals in stars to gas and the effects of the cluster potential on the overall evolution of the system. However, preliminary results indicate that the Fe abundance, for rich clusters, is at best only a weak function of temperature, luminosity, or mass (Mushotzky 1995; Ohashi et al. 1995). We anticipate that the *ASCA* data will allow a measurement of the abundance pattern over the factor of 5 range in X-ray temperature (1–5 keV) for which the lines of the abundant elements are strong and resolvable with *ASCA*.

We would like to thank Y. Tanaka and the *ASCA* team for the opportunity to participate in the *ASCA* PV data analysis effort and for their massive effort in preparing and operating *ASCA*, which has made this work possible. We would also like to thank K. Makishima for comments and discussions, Una Hwang for a careful reading of the manuscript, K. P. Singh for communication of results prior to publication and K. Borkowski for discussion of atomic physics codes.

REFERENCES

Antunes, A., Nagase, F., & White, N. E. 1994, ApJ, 436, L83
Arnaud, K. 1986, Ph.D. thesis, Cambridge Univ.
Arnaud, K., et al. 1994, presented at the HEAD Napa valley meeting
Arnaud, M. 1995, in Clusters of Galaxies, Proc. 29th Recontre de Moriond, ed. F. Durret, A. Mazure, & J. Tran Thanh Van (Gif-sur-Yvette: Editions Frontières), 211
Arnaud, M., Rothenflug, R., Boulade, O., Vigroux, L., & Vangioni-Flan, E. 1992, A&A, 254, 49
Awaki, H., et al. 1994, PASJ, 46, L65
Borkowski, K. 1995, private communication
Canizares, C., Clark, G. W., Jernigan, J. G., & Market, T. H. 1982, ApJ, 262, 33
Ciotti, L., Pellegrini, S., Renzini, A., & D'Ercole, A. 1991, ApJ, 376, 380
David, L., Forman, W., & Jones, C. 1991, ApJ, 359, 29
———. 1995, preprint
de Freitas Pacheco, J. A. 1993, ApJ, 403, 673
Dopita, M. 1991, Proc. Astron. Soc. Australia, 9, 234
Elbaz, D., Arnaud, M., & Vangioni-Flam, E. 1995, A&A, 303, 345
Fabian, A., Arnaud, K., Bautz, M., & Tawara, Y. 1994, ApJ, 436, L63
Franceschini, A., Mazzei, P., De Zotti, G., & Danese, L. 1995, ApJ, 427, 140
Grendreau, K., et al. 1995, PASJ, 47, 5
Gratton, L., & Ortolani, S., 1986, A&A, 169, 201
Hatsukade, I. 1989, Ph.D. thesis, Osaka Univ.
Hatsukade, I., Kawarabata, K., & Takenaka, K. 1995, paper presented at the 11th International Colloquium on UV and X-Ray Spectroscopy of Astrophysical and Laboratory Plasmas (Nagoya)
Henriksen, M., & Mushotzky, R. 1985, ApJ, 292, 441
Henry, R. B. C., Pagel, B., Chincarini, G. 1994, MNRAS, 258, 321
Hill, R. J., Madore, B. F., & Freeman, W. L. 1994, ApJ, 429, 204
Hu, E., Cowie, L., & Wang, Z. 1985, ApJS, 59, 44
Hughes, J., Butcher, J., Stewart, G., & Tanaka, Y. 1993, ApJ, 404, 611
Kaastra, J. 1995, private communication
Liedahl, D., Osterheld, A., & Goldstein, W. 1995, ApJ, 438, L115
Loewenstein, M., & Matthews, W. 1991, ApJ, 373, 445
Loewenstein, M., Mushotzky, R. F., Tamura, T., Ikebe, Y., Makishima, K., Matsushita, K., Awaki, H., & Serlemitsos, P. J. 1994, ApJ, 436, L75
Loewenstein, M., & Mushotzky, R. F. 1996, ApJ, 466, 695 (Paper II)
Luck, R., & Lambert, D. 1992, ApJS, 79, 303
Matteucci, F., & Francois, P. 1989, MNRAS, 239, 885
Mathews, W. G. 1989, AJ, 97, 42
Mewe, R., & Kaastra, J. 1992, Internal SRON-Leiden report
Mitchell, R., Ives, J., & Culhane, L. 1975, MNRAS, 175, 29
Mushotzky, R. 1984, Phys. Scr., T7, 157
———. 1995, in New Horizon of X-Ray Astronomy, ed. F. Makino & T. Ohashi. (Tokyo: Universal Academy), 243
Mushotzky, R., Holt, S. S., Boldt, E. A., Serlemitsos, P. J., & Smith, B. A. 1981, ApJ, 244, L47
Mushotzky, R. F., Loewenstein, M., M., Awaki, H., Makishima, K., Matsushita, K., & Matsumoto, H. 1994, ApJ, 436, L79
Mushotzky, R., Serlemitsos, P., Smith, B., Boldt, E., Holt, S. S. 1978, ApJ, 225, 21
Nomoto, K., Thielemann, F., & Yokoi, K. 1984, ApJ, 286, 644
Ohashi, T., Fukazawa, Y., Ikebe, Y., Ezawa, H., Tamura, T., & Makishima, K. 1995, in New Horizon of X-ray Astronomy, ed. F. Makino & T. Ohashi (Tokyo: Universal Academy), 234
Raymond, J., & Smith, B. A. 1977, ApJS, 35, 419
Renzini, A., Ciotti, L., D'Ercole, A., Pellegrini, S. 1993, ApJ, 419, 52
Rothenflug, R., Vigroux, L., Mushotzky, R., & Holt, S. S. 1984, ApJ, 279, 53
Russell, S. C., & Dopita, M. A. 1992, ApJ, 384, 508
Serlemitsos, P., Loewenstein, M. Mushotzky, R., Marshall, F., & Petre, R. 1993, ApJ, 413, 518
Serlemitsos, P., Smith, B., Boldt, E., Holt, S. S., & Swank, J. 1976, ApJ, 211, L63
Singh, K. P., White, N., & Drake, S. 1996, ApJ, 456, 766
Tanaka, Y., Inoue, H., & Holt, S. S. 1994, PASJ, 46, L37
Thielemann, F.-K., Nomoto, K., & Hashimoto, M. 1996, ApJ, 460, 408
Timmes, F. X., Woosley, S., & Weaver, T. A. 1995, ApJS, 98, 617
Tsuru, T. 1993, Ph.D. thesis, Univ. Tokyo
White, D., & Fabian, A. 1995, MNRAS, 273, 72
White R., Day, C., Hatsukade, I., & Hughes, J. 1994, ApJ, 433, 583
Woosley, S., & Weaver, T. 1986, ARA&A, 24, 205
Worthey, G., Faber, S. M., & Gonzalez, J. J. 1992, ApJ, 398, 69
Yamashita, K. 1992, in Frontiers of X-Ray Astronomy, ed. Y. Tanaka & K. Koyama (Tokyo: Universal Academy), 475